Chemical Engineering Science, Vol. 48, No. 8, pp. 1427–1436, 1993.
Printed in Great Britain.

0009–2509/93 $6.00 + 0.00

LIQUID DISTRIBUTION IN HORIZONTAL AXIALLY ROTATED PACKED BEDS

T. D. KARAPANTSIOS, N. A. TSOCHATZIDIS and A. J. KARABELAS†
Chemical Process Engineering Research Institute and Department of Chemical Engineering, Aristotle University of Thessaloniki, Univ. Box 455, GR 540 06 Thessaloniki, Greece

(*First received* 21 *May* 1992; *accepted for publication in revised form* 25 *September* 1992)

Abstract—This work is concerned with the distribution of the liquid phase in a partially filled horizontal packed bed. Liquid dispersion can be achieved by the rotary motion of the bed, acting in combination with gravity and surface tension forces. A conductance probe technique is employed to identify gross liquid distribution patterns. The technique involves specially designed parallel ring electrodes which are flush mounted on the bed wall to avoid packing disturbance. Steady-state experiments are conducted at several angular velocities and at various liquid fractions. Transient tests are also performed by keeping constant the angular acceleration rather than the angular velocity. For comparison, tests at the same liquid fractions are carried out in a conventional trickle bed setup using the same test section and probes. Conductance measurements, corresponding to nearly uniform distribution, from the above three configurations are in fair agreement. These data are also compared with the available theoretical expressions. Under steady rotation, there is a narrow range of small angular velocities favoring liquid dispersion. It is concluded that nearly uniform liquid distribution can be easily achieved in a horizontal axially rotated packed bed, over the entire range of liquid fractions of practical interest.

INTRODUCTION

At present there are no generally accepted methods for obtaining *uniform* liquid distribution throughout a packed bed in two-phase flow. Such a uniform distribution is very often required in processing (chemical reactors, contactors), in pilot experiments (with fluid–solid systems under well-controlled conditions) and in research activities (measurement of three-phase properties, calibrations, etc.). In the conventional *fixed* packed beds, axial and radial nonuniformities usually prevail due to the dynamic interaction of gas and liquid in the packing interstices (e.g. Hofmann, 1977). In fixed beds one can obtain nearly uniform liquid distribution only with small liquid and gas flow rates at which the so-called trickling flow prevails. Horizontal axially rotated packed beds seem to offer an attractive alternative for achieving nearly uniform liquid distribution (Karapantsios *et al.*, 1991).

The concept of rotating packed beds raised considerable interest, for countercurrent gas–liquid contact, during the past decade. Imperial Chemical Industries, U.K., were apparently the first ones to perform rather extensive tests on the so-called HIGEE packed-bed rotor. Unfortunately, little information was published in order to support U.S. patents (Ramshaw and Mallinson, 1981; Wen, 1983a, b). In the latter, a torus-like packed container was proposed with rotation about a vertical axis. Liquid sprayed into the inside cylindrical surface of the bed was forced to flow radially outward under the influence of the centrifugal field. Gas introduced at the outer bed surface could flow radially inward due to the imposed pressure gradient. Rotation of about 50–2000 rpm could give centrifugal acceleration of ~ 60 to $\sim 1000g$, causing a significant increase of the volumetric rate of mass transfer and of the throughput of each phase. It is possible that an increase of both the effective gas–liquid interfacial area and of the (liquid side) mass transfer coefficient contribute to such large mass transfer rates. Significant gas pressure drop and the difficulty of maintaining a low liquid holdup appear to be among the main disadvantages of the toroidal packed beds.

Munjal *et al.* (1989a, b) presented the results of modeling and experimental work on toroidal packed beds. It was shown that both the gas–liquid interfacial area and the gas–liquid mass transfer coefficient tend to increase with increasing speed of rotation. They also demonstrated the enhancement of volumetric mass transfer rates in the centrifugal field as compared to the conventional (gravity flow) packed beds. Keyvani and Gardner (1989) presented some additional experimental data.

Perhaps the only gas–liquid contact device, where some sort of *horizontal* rotated packed bed is used, is the so-called rotating biological contactor. The rotating bed is partially immersed in liquid, while the rest is exposed to the atmosphere. Air is trapped in the packing, thus facilitating liquid aeration and bio-oxidation. Reported applications include biological treatment of wastewater either from food production plants (Borghei, 1981) or from oil and chemical facilities (Hirata and Hosaka, 1991).

The main motivation behind the work presented here is the development of techniques for achieving uniform liquid distribution in the packing, under well-controlled conditions. A horizontal axially rotated packed bed (HARP) seems to offer this possibility without resorting to extreme conditions, e.g. high rotation speeds.

†Author to whom correspondence should be addressed.

In order to study the distribution of the liquid phase in a partially filled packed bed, a newly developed conductance technique (Tsochatzidis *et al.*, 1992) is employed. It is nonintrusive, as it relies on a pair of parallel ring electrodes mounted flash on the wall of the cylindrical vessel. This technique is characterized by satisfactory accuracy and stability for this kind of application. It is particularly sensitive to liquid distribution patterns in the cylindrical segment between the ring electrodes. Furthermore, with this technique one can discern the *gross* liquid distribution modes such as "annular", "stratified" and "uniformly distributed", as shown in Fig. 1, where the liquid fraction corresponds to the empty vessel. Clearly, the conductance in the case of uniformly distributed liquid is significantly smaller compared to that for the annular and stratified liquid pattern. This observation is essential for the interpretation of the data presented here.

Using the conductance technique, conditions favoring nearly uniform liquid distribution are identified. In the following sections, the results obtained under steady-state rotation are reported first, and then the data collected under transient conditions. Uniform liquid distribution under *steady* rotation is the prime target of this study. Data obtained under *transient* rotation (rolling) of the test section are employed for comparison with the steady-state measurements. Starting from a totally segregated liquid layer and keeping constant the angular acceleration, one can observe the evolution of the gross liquid distribution by monitoring the conductance.

Finally, the question is posed whether the liquid distribution achieved in HARP compares favorably with fluid dispersion in the conventional packed beds. To address this question, a comparison is made with the data obtained under trickling-flow conditions, using the same test section.

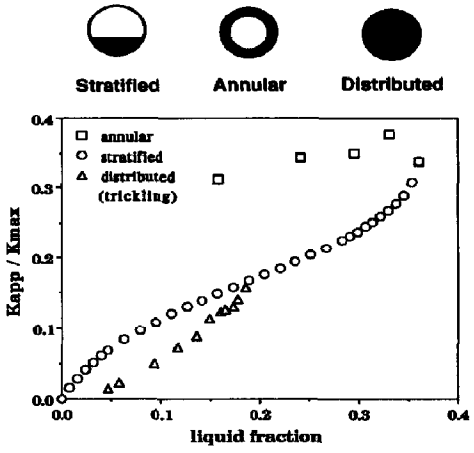

Fig. 1. Normalized conductance vs liquid fraction for various patterns of liquid distribution (Tsochatzidis *et al.*, 1992).

FORCES AFFECTING LIQUID DISTRIBUTION

This study deals with liquid dispersion in a *coarse* porous medium, i.e. a packing with characteristic dimension of passages (available to fluids) of a few millimeters. In order to characterize "liquid dispersion" in a vessel packed with such a porous medium, one must distinguish between even liquid distribution on a *large scale* (throughout the vessel) and uniform dispersion on a *small scale* (in the packing interstices). Thus, two length scales can be readily recognized, i.e. the vessel radius R and the particle radius r_p, representative of the large and small scale, respectively. It should be pointed out here that an even liquid distribution on the large scale may be associated with more than one dispersion pattern on the small scale.

The complexity of the physical system makes the hydrodynamics exceedingly difficult to study theoretically and it is not our intention to attempt it at present. Even the much simpler case, where only liquid and air are present inside a rotating vessel, has been only partially treated (Benjamin and Pathak, 1987). Here the main forces are recognized, which interact toward the establishment of a liquid distribution pattern. Their relative significance can be assessed by means of appropriate dimensionless numbers.

Of paramount importance is the Froude number (Fr), which is the ratio of centrifugal to gravitational forces. To achieve a nearly "annular" liquid distribution (almost solid-body type of rotation), a Froude number much larger than unity (i.e. large angular speed ω) is required. For very small values of Fr (i.e. small angular speed ω) gravity dominates, causing liquid settling (stratification) at the bottom of the vessel. In our application, centrifugal forces must be sufficiently large to counteract partially the gravitational forces and bring liquid to the *vessel top*, yet small enough to permit gravity to disperse that liquid. It appears, therefore, that one should expect liquid dispersion in the packed bed for Fr values of order not far from one. As shown in a subsequent section, the experimental data tend to support these arguments.

Table 1 includes (in addition to Fr) a few well-known dimensionless groups, such as the Bond (Bo), capillary (Ca) and Reynolds (Re) numbers, reflecting the relative significance of gravitational, capillarity, viscous and inertial forces. Both numbers for the packed bed and the empty vessel are presented for comparison. An effective rotational speed, $V_{\text{eff}} = \omega R$, is employed only as a rough measure of the liquid velocity relative to the rotating bed or empty tube. To obtain order-of-magnitude estimates, typical values of the various dimensionless numbers are listed in Table 1 for a rotation rate of 60 rpm, which is within the range of our tests.

It is clear that capillarity forces are far more significant [$Bo = O(1)$] for the bed than for the empty vessel and that they can compete effectively with gravity in the packing interstices. Surface tension forces are, thus, expected to play a dominant role in

Table 1. Typical values of force ratios for air–water mixtures in the rotated test section ($V_{eff} = \omega R$, $\omega = 2\pi n$, $n = 1$ Hz or 60 rpm)

Force ratio		Packed bed $L = r_p = 0.3$ cm	Empty tube $L = R = 7$ cm
$\frac{\text{Gravitational}}{\text{Capillarity}}$,	$Bo = \frac{(\varrho_L - \varrho_G)gL^2}{\sigma}$	1.2	6.7×10^2
$\frac{\text{Viscous}}{\text{Capillarity}}$,	$Ca = \frac{\mu V_{eff}}{\sigma}$	6.1×10^{-3}	6.1×10^{-3}
$\frac{\text{Inertial}}{\text{Viscous}}$,	$Re = \frac{\varrho_L V_{eff} L}{\mu}$	1.3×10^3	3.1×10^4
$\frac{\text{Centrifugal}}{\text{Gravitational}}$,	$Fr = \frac{\varrho_L V_{eff}^2}{(\varrho_L - \varrho_G)gR}$	0.3	0.3

promoting dispersion during transient bed rotation and in maintaining a nearly uniform liquid distribution under steady rotation.

The influence of viscous forces in the rotating test section is evidently insignificant compared to capillarity and inertial forces [$Ca \ll O(1)$, $Re \gg O(1)$]. It is interesting that Karweit and Corrsin (1975), in their study of rotating tubes partially filled with water, also conclude that viscosity effects are unimportant.

As a final note, the following physical picture emerges from the above order-of-magnitude estimates: The centrifugal forces, partially overcoming gravity, are responsible for bulk liquid movement. In turn, gravity tends to promote liquid distribution on the large scale (R), while capillarity forces enhance liquid dispersion on the length scale of the packing interstices. It is necessary at this point to examine experimentally the liquid distribution resulting from the complex interplay of the aforementioned forces.

STEADY ROTATION

Apparatus and procedure

The experimental setup is shown schematically in Fig. 2. The main component is a transparent cylindrical Plexiglas vessel of inner diameter 14 cm and length 20 cm. Circular Plexiglas plates are flanged tight to the vessel at both ends. Two circular steel disks are bolted on the Plexiglas plates. The vessel is supported horizontally by steel shafts which are fixed (welded) centrally onto the steel plates, at both ends. Each shaft is mounted in roller bearings to provide a rigid support and ensure good alignment. The shaft at one end is connected to a variable-speed motor through a flexible coupling. The entire assembly (except for the motor) is fastened onto a heavy steel base plate, lying on a rubber sheet. The motor rests on thick rubber supports with adjustment screws, that allow an accurate alignment of the motor shaft with the rest of the rotating parts.

The rotation rate is continuously variable over the range 20–90 rpm and controlled by means of a mechanical built-in reducer. The angular velocity of the bed is measured by a stroboscopic digital tachometer. The overall accuracy in attaining a specific rotation rate by the gearbox (including the tachometer measurement) is better than 0.1 rpm, the major error being attributed to the reducer.

Glass spheres of radius $r_p = 0.3$ cm are used as packing material, giving an aspect ratio $R/r_p = 23.3$, which is rather typical for packed beds. Unpolished glass is employed to avoid wetting problems at low liquid fractions (Hofmann, 1977). Special care is taken when filling the vessel with particles to achieve uniformly close-packed conditions. More details of the procedures are given elsewhere (Tsochatzidis and Karabelas, 1991). The resulting void fraction is $\varepsilon = 0.36$. Measured quantities of tapwater are injected, or withdrawn through taps. The water is filtered to remove particles larger than 5 μm. By continuously monitoring water conductivity and reducing it to a reference value, the effect of temperature fluctuations on the measurements is effectively removed.

Conductance measurements are made by means of three ring electrodes (strips) flush mounted onto the inner surface of the test section (Fig. 2). The width S of the strips is 3 mm. Combinations of two ring electrodes are employed, having characteristic separation distances $D_e = 3$ and 6 cm, as shown in Fig. 2. The distance D_e must be carefully selected in order to obtain meaningful data. Criteria for such a selection may be based on the volume-averaging approach of modeling porous media (e.g. Carbonell and Whitaker, 1984). The size of the probe averaging volume, i.e. the required minimum packing volume surrounding a probe, must be large enough to average porosity undulations (due to the finite particle size) yet small enough to preserve the local character of the measurement. Celmins (1988) while working with gas–particle mixtures showed that the above "representative elementary volume" criteria are satisfied if the averaging volume contains at least 60–150 particles. The electrode spacing employed here ($D_e = 3$ and 6 cm) is in accord with the above criteria. Moreover, the ring electrodes are at a distance greater than 7 cm from either end of the bed, which is considered sufficient to avoid end effects, as shown elsewhere (Tsochatzidis *et al.*, 1992).

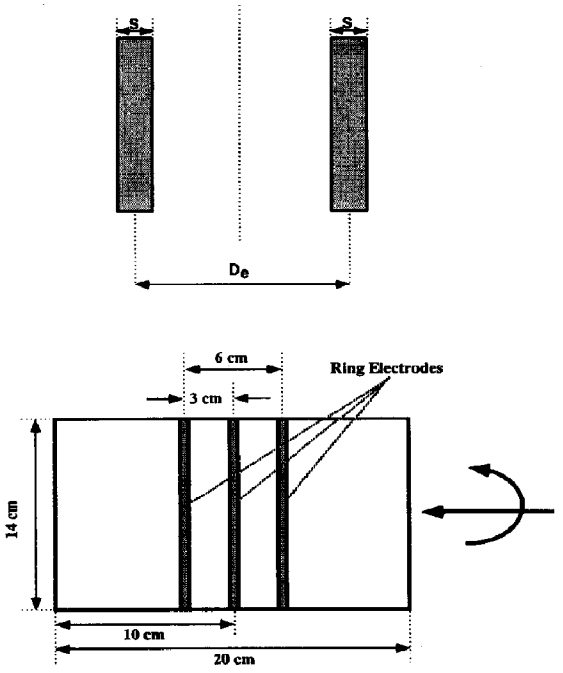

Fig. 2. Schematic of probe geometry and cylindrical apparatus.

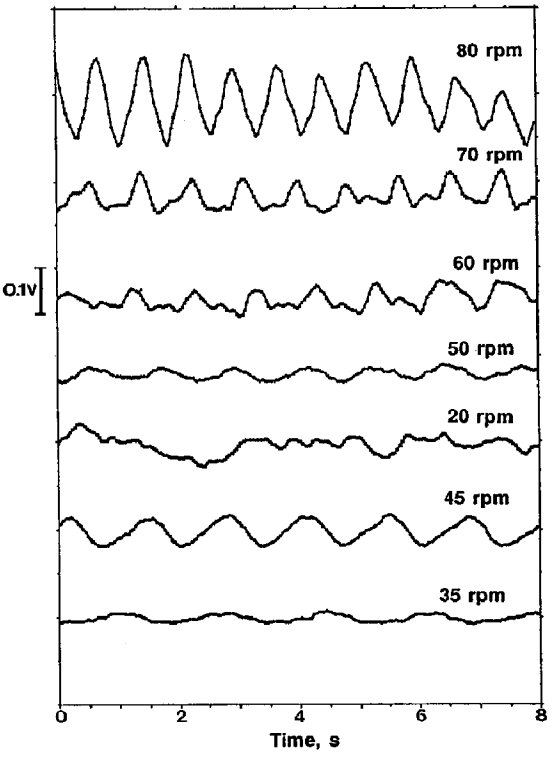

Fig. 3. Probe response under steady rotation; electrode spacing $D_e = 3$ cm, $\beta = 0.05$.

Electrical connection of the rotating ring electrodes is achieved by means of copper ribbons (one for each ring), glued circumferentially onto the outer Plexiglas surface. Small screws in the vessel wall connect the inner wetted electrodes with the external copper ribbons. The latter are in good contact with special springs, in the form of hard metal strips (one for each electrode), fixed at one end on the base plate and pressed at their free end on the rotating test section.

The signal from each pair of probes is fed to a special electronic analyzer similar to that reported by Karapantsios *et al.* (1989), where details are also given about the electronic circuit and the calibration. The voltage output of the analyzer is converted to equivalent conductance using a calibration curve. The signal from the electronic unit is collected and stored in a microcomputer. With the bed in steady rotation, 2 or 3 min are usually allowed before data collection. Data are acquired over a period of 20 s with a 50 Hz sampling frequency, which proved to be more than adequate for these experiments.

Results

Typical voltage traces from one electrode pair (with $D_e = 3$ cm) are shown in Fig. 3 corresponding to a liquid volume fraction $\beta = 0.05$. Each trace is obtained with a fixed rotation rate. Similar curves are obtained with the other electrode pair ($D_e = 6$ cm) and with various liquid fractions.

All traces display periodic fluctuations which may be attributed to inherent features of the liquid motion rather than to imperfections of the experimental setup. It is pointed out that the origin of the vertical coordinate in Fig. 3 is arbitrarily floating, so that only the magnitude of undulations conforms to the same scale. However, the sequence of the drawn curves corresponds to their relative signal level. The amplitude of these undulations tends to grow with the rotation rate up to $n = 30$–40 rpm, reaching an almost constant value at higher speeds. However, the intensity (i.e. standard deviation over mean voltage) is always very small (of order 0.01), indicating that the respective undulations are relatively insignificant. A negligible amount of random noise, which is evident in each trace, may be due to minor local nonuniformities on the electrodes' surface. Statistical analysis of the traces—coefficients of skewness, $a_3 \cong 0$, and of kurtosis, $a_4 \cong -0.5$—indicates that the signal is almost evenly distributed about its mean value. Furthermore, Fast Fourier Transform analysis demonstrates that the dominant frequency in the traces is practically equal to the frequency of rotation and (in some cases) to its subharmonics. Finally, the autocorrelation function gives plots of typical narrow-band frequency signals (Bendat and Piersol, 1986). Extensive testing shows very good reproducibility of the measured conductance. Moreover, no hysteresis effects are detected under different modes of executing the experiments, i.e. decreasing or increasing the rotation rate, shutting down the system after a run and restarting it from rest.

Some anomalies and deviations from the above behavior are displayed by data taken at high liquid fractions, i.e. close to, and above, $\beta = 0.30$. In these cases, the output signal appears to drift, slowly increasing with time, for a typical test period of about 20 s. Moreover, hysteresis effects are evident which may be due to multiple stable steady states, developing during rotation in the smaller scale (interstices). This behavior (displayed by both probes) may be caused by air pockets or air bubbles trapped in the packing interstices, which are difficult to relocate by increasing the speed of rotation. In support of this explanation is the fact that after some runs it proved almost impossible to inject more water into the bed to achieve a liquid fraction greater than $\beta = 0.32$. Obviously, trapped *air* bubbles in the packing interstices did not permit further liquid addition. In general, a liquid fraction $\beta \cong 0.30$ seems to represent the upper limit of easily reproducible data taken with the conductance technique. It may also correspond to the upper limit for possible practical applications.

Figures 4 and 5 present the experimental results, plotted as time-averaged, normalized conductance vs frequency of rotation for the two probe pairs. The K_{max} value corresponds to the apparent conductance measured when the *empty* test section is filled with water. Normalizing the data with K_{max} allows one to eliminate errors introduced by variations of the specific liquid conductivity.

The data taken with the two pairs of probes ($D_e = 3$ and 6 cm) are in very good agreement throughout the range of speeds of rotation examined. Of particular interest here is the fact that all the curves (corresponding to constant β) display a minimum for rotation rates in the narrow range 30–40 rpm. This minimum, as discussed in the Introduction in connection with Fig. 1, is indicative of the most uniform liquid distribution attainable under rotation for a constant liquid fraction β.

The curves corresponding to $\beta = 0.29$ do not exhibit a clear minimum, but rather a tendency for gradually increasing conductance with rate of rotation. This trend at high β, as well as hysteresis effects discussed earlier, may be due to poor distribution of trapped air bubbles throughout the packing. It is also noted that for an even greater liquid fraction ($\beta = 0.32$, Fig. 4) the measured average conductance has a constant value, independent of rotation rate.

It may be pointed out here that the rotation rate associated with the nearly uniform liquid distribution under steady rotation (i.e. $n = 30$–40 rpm, Figs 4 and 5) corresponds to a Froude number of 0.07–0.13, i.e. $Fr = O(10^{-1})$. As discussed in the preceding sections, this implies that gravity plays a significant role in the *gross* distribution of liquid in the packing.

Figure 6 presents the minimum K_{app}/K_{max} values corresponding to each data set (such as those of Figs 4 and 5) for constant mean liquid fraction, indicating nearly uniform liquid distribution. The results from both electrode pairs are very close, especially in the intermediate liquid fractions. Deviations appear for fractions greater than 0.25, at which anomalous behavior was observed. The discrepancy between the data points at $\beta = 0.36$ is particularly noteworthy. These points were obtained by filling up the test section slowly to ensure that no air bubbles were left in the packing. Furthermore, the reproducibility of each data point was checked repeatedly and found to

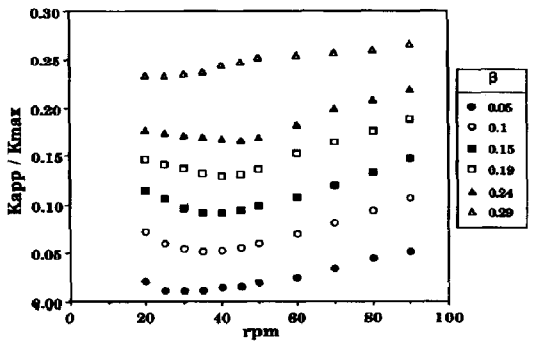

Fig. 5. Normalized conductance vs rate of rotation for various mean liquid fractions, β. Large electrode spacing, $D_e = 6$ cm.

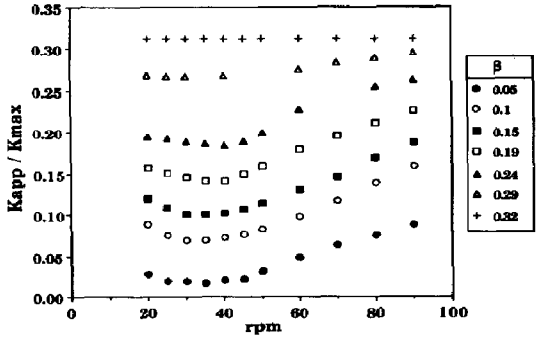

Fig. 4. Normalized conductance vs rate of rotation for various mean liquid fractions, β. Small electrode spacing, $D_e = 3$ cm.

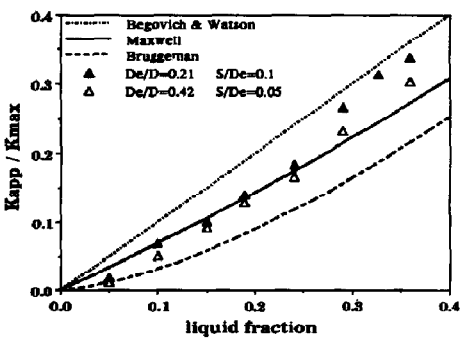

Fig. 6. Normalized conductance vs liquid fraction, β, under conditions of uniform liquid distribution.

be better than 99%. Thus, the 11% difference of the two points (obtained from two electrode combinations) is, at first glance, surprising. An explanation may be based on the voidage "fluctuations" adjacent to the cylindrical wall (e.g. Govindarao *et al.*, 1990) which apparently can influence the measured conductance. Ring electrodes spaced 6 cm apart are expected to be less sensitive to such local non-uniformities (compared to electrodes with $D_e = 3$ cm) since a better averaging is achieved leading to a more representative measurement (Tsochatzidis *et al.*, 1992).

In Fig. 6. a comparison is also made with the following expressions for apparent conductivity:

Maxwell (1881)

$$\frac{\gamma}{\gamma_L} = \frac{2\beta}{3-\beta}$$

Bruggeman (1935)

$$\frac{\gamma}{\gamma_L} = \beta^{3/2}$$

Begovich and Watson (1978)

$$\frac{\gamma}{\gamma_L} = \beta.$$

As is well known, for uniformly distributed systems the ratio γ/γ_L is equal to the ratio K_{app}/K_{max} determined in this work. The measured normalized conductance falls between predictions based on Bruggeman's and Begovich and Watson's expressions for the effective electrical conductivity of the composite medium, throughout the range of liquid fractions. For low and intermediate liquid fractions the data agree quite well with the Maxwell expression, with the exception of one point (at $\beta = 0.05$), which is closer to the Bruggeman predictions. It should be pointed out that the Maxwell and Bruggeman equations were developed for media with a large fraction of the conducting continuous phase, i.e. much larger than $\beta = 0.40$. However, they are applied here to a different range of β values. For liquid fractions above 0.28, the data variation extends between the Maxwell and the Begovich and Watson expressions. The latter was originally developed for three-phase fluidized beds with liquid holdup between 0.1 and 0.5.

TRANSIENT ROTATION

Apparatus and procedure

The test section was essentially the same as that of the previously outlined steady-state experiments (Fig. 2). To facilitate the transient experiments, only a minor modification was made, i.e. the copper ribbons were replaced by long ($\sim$3 m) lead wires connecting directly the ring electrodes with the electronic analyzer.

As outlined in the Introduction, the objective of the transient tests was to study liquid distribution under nearly constant angular *acceleration*, rather than constant angular velocity. Rolling of the test section on a flat ramp (235 cm long, 23 cm wide) was selected as the most convenient technique to achieve this goal. The cylindrical test section was allowed to move smoothly on two parallel aluminum guides, of an L-shaped cross section. These guides were mounted on the ramp so that they formed a rail path of constant width, inside which the rolling section had a loose fit. The angle of ramp inclination was adjustable, thus permitting operation under various accelerations. Data for three angles of inclination ($\theta = 2.2$, 4.4 and 7.5°) were obtained. These relatively small angles were selected to avoid sliding.

Glass spheres of 3 mm nominal radius were again used as packing material, with an average void fraction $\varepsilon = 0.36$. In the transient experiments only one ring electrode pair with $D_e = 3$ cm was employed. Data were collected with 100 Hz sampling frequency for periods of 5–6 s.

A typical experiment started with the water settled in the bed ("stratified" pattern). The test section was then allowed to roll freely down the ramp, at a preselected angle of inclination θ. During this rolling, conductance data were collected, while timing the motion and making visual observations through the transparent side plates.

Results

Figure 7 presents schematically the evolution of liquid gross distribution patterns as perceived by means of observations through the side plates. As a typical case, it is assumed that the bed is less than half filled. The letters A, B, C . . . are used to identify the possible intermediate liquid distribution *states* rather than to mark locations along the ramp. Shaded areas

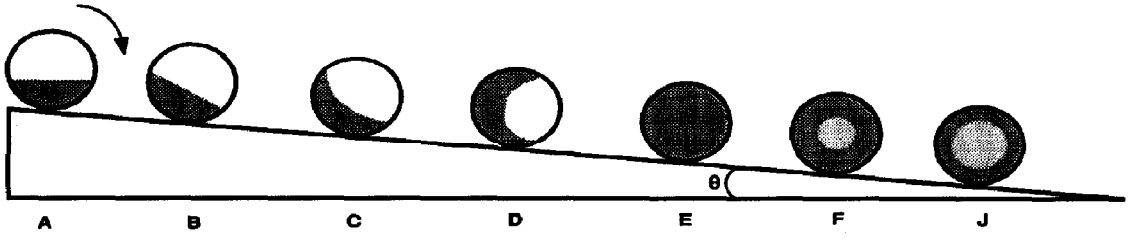

Fig. 7. Observations made during tansient rotation (rolling). Sketch of possible liquid distribution patterns.

designate dispersed liquid, the packing being omitted for clarity. Admittedly, the last two sketches (F and J) depict only impressions of a liquid distribution pattern difficult to discern visually.

These observations suggest that, during transient rotation, a condition of nearly uniform liquid distribution (state E, Fig. 7) may be attained, before increased centrifugal forces drag the fluid toward the cylindrical wall of the vessel. Similar distribution regimes have been reported by Kelbert and Royere (1991) for a charge of particles in a kiln rotating with an increasing velocity. The evolution of the liquid distribution patterns is evidently the result of a continuous interplay among gravitational, surface tension, inertial and viscous forces, as outlined in a preceding section. With increasing centrifugal acceleration, inertial effects may gradually dominate over the others.

In order to estimate the angular acceleration achieved in the tests, it is assumed that during rolling the bed has a uniform density and that it does not slide. The validity of the former assumption is supported by the fact that the weight of the liquid is, in most cases, less than 10% of the total weight of the rolling bed. Moreover, some degree of liquid dispersion appears to be attained quite rapidly. The "uniform density" approximation is tested by comparing the measured and the predicted travel times for the bed to cover the length of the ramp. A fairly satisfactory agreement is obtained, particularly for the smaller inclinations, i.e. $\theta = 2.2$ and 4.4°. The computed bed angular accelerations for $\theta = 2.2$, 4.4 and 7.5° are 3.6 rad/s^2 (or 34.2 rpm/s), 7.2 rad/s^2 (68.4 rpm/s) and 12.2 rad/s^2 (116.5 rpm/s), respectively. The corresponding translational accelerations of the bed are 0.25, 0.5 and 0.85 m/s^2.

Voltage traces are presented in Figs 8 and 9 for several liquid volume fractions and two angles of inclination, namely, 2.2 and 4.4°. The signal appears to be very smooth, with a low noise level, and its reproducibility is excellent. During a short startup period of rolling, no detectable signal change occurs. This period is followed by a steady signal reduction toward a minimum value (marked with an arrow in Fig. 8). The latter is considered indicative of the *best liquid distribution* attainable for a set of parameters θ and β, as is also the case in the steady-state experiments. After the first minimum, the signal tends to increase again towards values considerably higher (in most cases) than the initial value corresponding to "stratified" pattern. This increase may be indicative of a pseudo-annular type of pattern.

Almost all traces demonstrate some sort of oscillatory pattern of variable period and amplitude. Such oscillations are quite clear in the small liquid fractions. The signals for $\beta = 0.29$ show an imperceptible

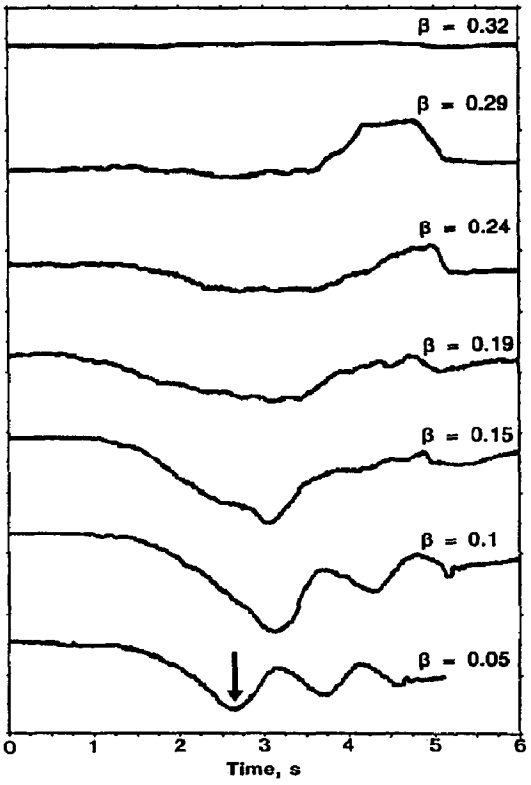

Fig. 8. Probe response to bed acceleration (rolling, $\theta = 2.2°$).

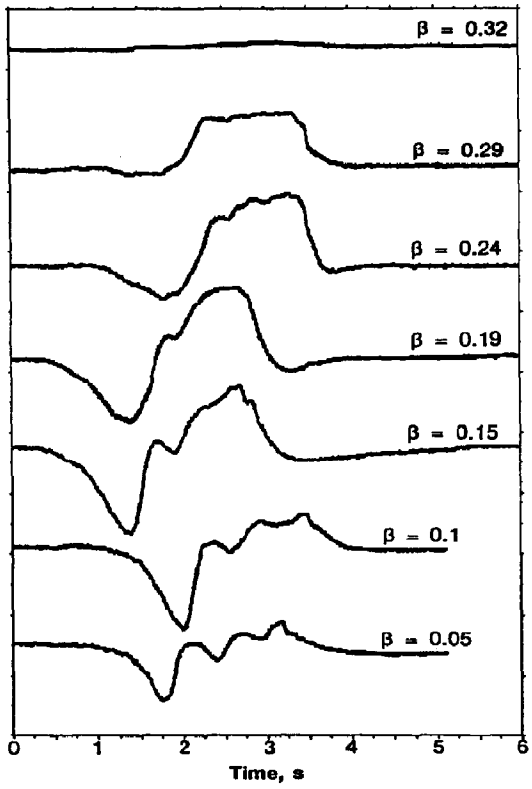

Fig. 9. Probe response to bed acceleration (rolling, $\theta = 4.4°$).

drop first, followed by a plateau, which might be associated with an annular type of pattern. The signal for $\beta = 0.32$ is nearly flat, displaying a behavior similar to that in the steady-state tests.

Figure 10 depicts reduced apparent conductance values corresponding to the first minimum of the traces, such as those of Figs 8 and 9. The data obtained with $\theta = 2.2$ and 4.4° are quite close, the majority falling in between Maxwell's and Bruggeman's predictions. The points for $\theta = 7.5°$ and small liquid fractions ($\beta < 0.10$) are quite high and possibly not representative of the assumed nearly uniform distribution. It is suspected that sliding of the test section may contribute to this discrepancy.

TRICKLING FLOW

Apparatus and procedure

An additional set of experiments were performed in a gravity-fed packed bed, operated in the trickling-flow regime. The latter is usually considered to represent uniform liquid distribution only when specific requirements are met. In particular, the bed aspect ratio must be larger than 20 to minimize wall effects. Furthermore, a liquid distributor and sufficient column height must be employed to avoid maldistribution of the liquid (Herskowitz and Smith, 1983; Hofmann, 1977).

To this end, tests were carried out under ambient conditions in a conventional trickle bed setup, similar to that described by Tsochatzidis and Karabelas (1991). The same test section of the HARP unit (aspect ratio 23.3) became part of a tall (1.24 m) vertical packed bed. Air and water were used in the tests, flowing cocurrently downwards. Water was sprayed uniformly on the top of the packing through a perforated distributor and air was introduced by means of another perforated tubular section. Water was supplied in the range 1.483–29.790 kg/m^2 s while the gas flow rate was held constant at 0.055 kg/m^2 s. Experimental data by Herskowitz and Smith (1978) with a system similar to ours showed that indeed nearly uniform distribution prevails.

Liquid fractions were measured using a technique based on electrically operated "quick-closing valves". The average liquid fraction in the column was determined by draining the liquid trapped (after closing the valves) for about 10–15 min. Liquid fractions were independently obtained under various liquid flow rates, while the signal from the conductance probe was recorded simultaneously.

Results

In Figure 11, liquid fractions are plotted against liquid mass flow rate. Data reported by Levec *et al.* (1986, Fig. 3) are also shown for comparison, as well as predictions made by Ellman *et al.* (1990). The data of Levec *et al.* correspond to a bed with the same packing characteristics as our system, and no gas flow. On the other hand, the Ellman *et al.* correlation is deduced from numerous data covering a wide range of experimental conditions and parameters. The dashed lines depicted in Fig. 11 mark an error limit of 50% in the predictions, as indicated in that work.

Upon inspection of Fig. 11, it is evident that there is a remarkable agreement between the different data sets and a fair agreement between the data and the Ellman *et al.* correlation. The latter seems to perform better for trickling flow under relatively high liquid rates. In conclusion, the new trickling-flow data are accurate and evidently representative of a nearly uniform liquid distribution in the bed.

COMPARISON OF TECHNIQUES FOR LIQUID DISTRIBUTION

A comparison of the data obtained from both modes of bed rotation with measurements made in the trickle bed is now in order. The data from all these tests are plotted in Fig. 12. For both steady and transient rotation only the minimum values obtained at each liquid fraction are presented, regardless of the rotation rate or the inclination. Predictions due to Maxwell, Bruggeman, and Begovich and Watson are also plotted in this figure. The transient experiments

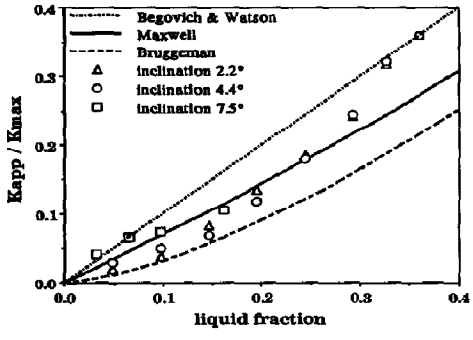

Fig. 10. Data from transient experiments. Normalized conductance vs liquid fraction under conditions of nearly uniform distribution.

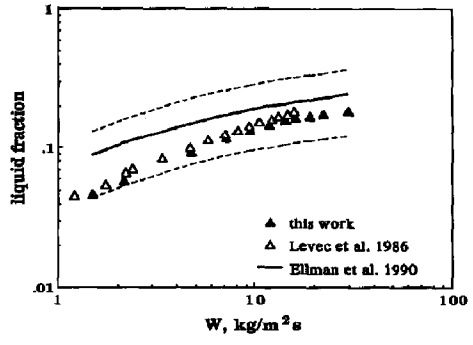

Fig. 11. Comparison between liquid fraction data of this work with data and predictions from literature, for the trickling-flow regime.

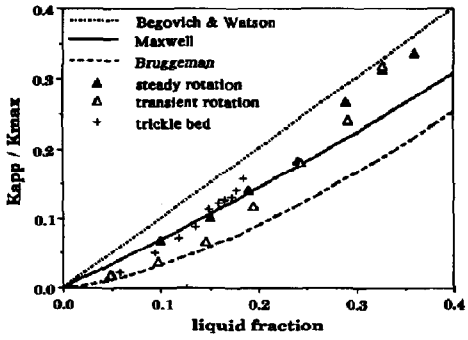

Fig. 12. Nearly uniform liquid distribution achieved with three different modes of packed-bed operation.

give the smallest values of the reduced conductance K_{app}/K_{max}, suggesting that (over a short time period) one may obtain the best liquid distribution. Trickling flow seems to result in a liquid distribution similar to that obtained by steady-state rotation only for liquid fractions β smaller than 0.15. However, for β greater than $\sim$0.18 trickling flow does not exist and flow nonuniformity prevails in fixed beds.

The data (Fig. 12) clearly demonstrate the merits of a rotating bed (as compared to the conventional vertical fixed beds) in achieving a nearly uniform liquid distribution practically over the *entire range* of liquid fractions. In fact, HARP appears to be a convenient method for obtaining liquid uniformity at relatively high loads, i.e. for β greater than 0.18.

DISCUSSION

It is interesting that, under steady rotation, nearly uniform distribution is obtained over a narrow range of small angular velocities (30–40 rpm). At these rotation rates centrifugal forces are apparently roughly comparable to gravitational forces. This seems to be a necessary condition for *gross* liquid distribution. Surface tension forces tend to promote liquid distribution on a *small* scale, i.e. in the interstices.

As pointed out in a preceding section, an even liquid distribution on the large scale (throughout the rotating packed bed) may be associated with more than one dispersion modes on the small scale (interstices). These modes appear to be stable under steady rotation. Thus, using these arguments, one may explain the behavior of some data (Figs 3, 4 and 5, especially at high liquid fractions) displaying hysteresis effects or a tendency for increasing conductance over a finite time period. Obviously, the experimental technique employed here cannot provide information relating to dispersion on the small length scale.

The satisfactory agreement between the data obtained in two entirely different systems (i.e. under steady rotation and in a trickle bed setup) reinforces our confidence in the conclusions reached here on nearly uniform liquid distribution. It is noteworthy in this respect that under steady rotation one can easily disperse the liquid essentially *throughout* the range of liquid fractions β, something difficult to achieve by other means. Furthermore, the extra degree of freedom (rotation) for achieving liquid dispersion in HARP can be implemented with relatively simple equipment. Therefore, HARP may hold distinct advantages over fixed packed beds for specific process requirements, e.g. handling sensitive fluids, controlling residence time, carrying out gas–liquid reactions with a fixed holdup, etc.

In conclusion, the validity of a new method for liquid distribution inside a packed bed is demonstrated in this study. It remains, of course, to clarify several questions, especially those relating to scaleup, and to the degree of dispersion on the small scale. Work in that direction is underway.

Acknowledgements—Financial support by the Commission of European Communities (Contract No. JOUG-0005-C) is gratefully acknowledged. Helpful discussions with Mr S. Mastrogeorgopoulos are appreciated.

NOTATION

a_3	coefficient of skewness
a_4	coefficient of kurtosis
D_e	ring electrodes separation distance, cm
g	acceleration due to gravity, cm/s^2
K_{app}	apparent conductance of bed partially filled with water, μS
K_{max}	apparent conductance of empty tube filled with water, μS
L	characteristic length, cm
n	rotational frequency, Hz
R	bed radius, cm
r_p	particle radius, cm
S	ring electrodes width, mm
V	translational velocity, cm/s
V_{eff}	effective translational velocity, cm/s
W	liquid mass flow rate, kg/m^2 s

Greek letters

β	liquid volume fraction
γ	apparent conductivity of bed partially filled with water, μS/cm
γ_L	liquid conductivity, μS/cm
ε	void fraction
θ	angle of inclination, deg
μ	viscosity, g/cm s
ϱ	density, g/cm^3
σ	surface tension, dyn/cm
ω	angular speed, rad/s

Dimensionless groups (Perry and Chilton, 1973)

Bo	Bond number $[=(\varrho_L-\varrho_G)L^3g/\sigma L]$
Ca	capillary number $[L\mu V/\sigma L]$
Fr	Froude number $[=(\varrho_L L^3V^2/R)/(\varrho_L-\varrho_G)L^3g]$
Re	Reynolds number $[=\varrho_L L^2V^2/L\mu V]$

REFERENCES

Begovich, J. M. and Watson, J. S., 1978, An electroconductivity technique for the measurement of axial variation of holdups in three-phase fluidized beds. *A.I.Ch.E. J.* **24**, 351–354.

Bendat, J. S. and Piersol, A. G., 1986, *Random Data: Analysis and Measurement procedures*. Wiley–Interscience, New York.

Benjamin, T. B. and Pathak, S. K., 1987, Cellular flows of a viscous liquid that partly fills a horizontal rotating cylinder. *J. Fluid Mech.* **183**, 339–420.

Borghei, S. M., 1981, Treatment of the effluent of a glucose production plant using a rotating biological packed bed. *Process Biochemistry* 29–34.

Bruggeman, D. A. G., 1935, Calculation of different physical constants of heterogeneous substances. *Ann. Phys.* **24**, 636–679.

Carbonell, R. G. and Whitaker, S., 1984, Heat and mass transfer in porous media, in *Fundamentals of Transport Phenomena in Porous Media* (Edited by J. Bear and Y. Corapcioglu), pp, 121–198. Nijhoff, The Hague, The Netherlands.

Celmins, A., 1988, Representation of two-phase flows by volume averaging. *Int. J. Multiphase Flow* **14**, 81–90.

Ellman, M. J., Midoux, N., Wild, G., Laurent, A. and Charpentier, J. C., 1990, A new, improved liquid hold-up correlation for trickle-bed reactors, *Chem. Engng Sci.* **45**, 1677–1684.

Govindarao, V. M. H., Subbana, M., Rao, A. V. S. and Ramrao, K. V. S., 1990, Voidage profile in packed beds by multi-channel model: effects of curvature of the channels. *Chem. Engng Sci.* **45**, 362–364.

Herskowitz, M. and Smith, J. M., 1978, Liquid distribution in trickle-bed reactors. *A.I.Ch.E. J.* **24**, 439–450.

Herskowitz, M. and Smith, J. M., 1983, Trickle-bed reactors: a review. *A.I.Ch.E. J.* **29**, 1–17.

Hirata, A. and Hosaka, Y., 1991, Biological treatment of waste-water from the washing of oil and chemical drums in a rotating biological contactor. *Int. Chem. Engng* **31**, 128–133.

Hofmann, H., 1977, Hydrodynamics, transport phenomena, and mathematical models in trickle-bed reactors. *Int. chem. Engng* **17**, 19–27.

Karapantsios, T. D., Paras, S. V. and Karabelas, A. J., 1989, Statistical characteristics of free falling films at high Reynolds numbers. *Int. J. Multiphase Flow* **15**, 1–21.

Karapantsios, T. D., Tsochatzidis, N. A. and Karabelas, A. J., 1991, Liquid distribution in horizontal axially rotated packed beds. Paper presented at AIChE Annual Meeting, Los Angeles, CA, 17–22 November (Paper No. 202h).

Karweit, M. J. and Corrsin, S., 1975, Observation of cellular patterns in a partly filled, horizontal, rotating cylinder. *Phys. Fluids* **18**, 111–112.

Kelbert, F. and Royere, C., 1991, Lateral mixing and heat transfer in a rolling bed. *Int. chem. Engng* **31**, 441–449.

Keyvani, M. and Gardner, C. N., 1989, Operating characteristics of rotating beds. *Chem. Engng Prog.* 48–52.

Levec, J., Saez, A. E. and Carbonell, R. G., 1986, The hydrodynamics of trickling flow in packed beds. Part II. Experimental observations, *A.I.Ch.E. J.* **32**, 369–380.

Maxwell, J. C., 1881, *A Treatise on Electricity and Magnetism*. Clarendon, Oxford.

Munjal, S., Dudukovic, M. P. and Ramachandran, P., 1989a, Mass-transfer in rotating packed beds—I. Development of gas–liquid and liquid–solid mass-transfer correlations. *Chem. Engng Sci.* **44**, 2245–2256.

Munjal, S., Dudukovic, M. P. and Ramachandran, P., 1989b, Mass-transfer in rotating packed beds—II. Experimental results and comparison with theory and gravity flow. *Chem. Engng Sci.* **44**, 2257–2268.

Perry, R. H. and Chilton, C. H., 1973, *Chemical Engineer's Handbook*, 5th Edition. McGraw-Hill, New York.

Ramshaw, C. and Mallinson, R. H., 1981, Mass transfer process. U.S. Patent 4,283,255.

Tsochatzidis, N. A. and Karabelas, A. J., 1991, Hydrodynamic properties of pulses in trickle beds. In *Proceedings of the 2nd World Conference on Experimental Heat Transfer, Fluid Mechanics and Thermodynamics* (Edited by J. F. Keffer, R. K. Shah and E. N. Ganic), pp. 1515–1522. Elsevier, Amsterdam.

Tsochatzidis, N. A., Karapantsios, T. D., Kostoglou, M. V. and Karabelas A. J., 1992, A conductance probe for measuring liquid fraction in pipes and packed beds. *Int. J. Multiphase Flow* **18**, 653–667.

Wen, J. M., 1983a, Centrifugal gas–liquid contact apparatus. U.S. Patent 4,382,045.

Wen, J. M., 1983b, Centrifugal gas–liquid contact apparatus. U.S. Patent 4,382,900.